JOURNAL OF MATERIALS SCIENCE **39** (2004) 4219–4230

Interaction of iron-chromium alloys containing 10 and 25 mass% chromium with liquid aluminium

Part II *Formation of intermetallic compounds*

K. BARMAK
Department of Materials Science and Engineering, Carnegie Mellon University, Pittsburgh, PA 15213, USA
E-mail: katayun@andrew.cmu.edu
URL: http://materials.cmu.edu/barmak

V. I. DYBKOV
Department of Physical Chemistry of Inorganic Materials, Institute for Problems of Materials Science, Kyiv 03180, Ukraine
E-mail: v@dybkov.kiev.ua, dep6@materials.kiev.ua
URL: http://users.i.com.ua/~dybkov/V/index.html

Two intermetallic layers Fe_2Al_5 and Fe_2Al_7 occur at the interface between the iron-chromium alloys containing 10 and 25 mass% Cr and the saturated aluminium melt at 700°C. Under conditions of simultaneous dissolution in pure liquid aluminium only the Fe_2Al_5 phase forms an adherent continuous layer, while the Fe_2Al_7, $FeAl_3$, $FeAl_6$, $CrAl_7$ and other phases exist as inclusions in the aluminium matrix. Dissolution of the Fe–Cr alloy base into pure aluminium causes a three-fold decrease in layer thickness compared with the case where no dissolution occurs. A simple equation for evaluating the Fe_2Al_5 layer thickness during dissolution is proposed. Making the Fe–Cr alloy-to-aluminium transition joints, with the mechanical strength of the joint greater than or equal to that for pure aluminium (70–80 MPa), appears to be feasible.

1. Introduction

Many technologically important processes such as hot-dip protective coating of solid surfaces, soldering or welding of dissimilar metals and alloys, sintering in the presence of the liquid phase, etc., are known to be based on the interaction of a solid metal or alloy with a liquid-metal melt. During the interaction, the solid base dissolves in the melt, while the intermetallic compounds are formed at or in the vicinity of phase interfaces. The formation of thick brittle intermetallic layers strongly deteriorates the mechanical strength of the transition zone between dissimilar metals or alloys. This is especially the case with the couples formed by iron or its alloys with aluminium. Amongst those, the Fe–Cr alloy-aluminium couple is known to be one of the most unfavourable with respect to the weakness of the joint, due to the occurrence of the intermetallics both at the phase interface in the form of a relatively thick continuous layer and in its vicinity in aluminium as the aggregation of coarse grains. The former occurs in the course of a chemical reaction, while the latter are formed during cooling-down the aluminium melt. When joining such materials, the surface of a more refractory metal or alloy must first be plated with another metal in order to prevent, to a greater or a lesser extent, the formation of intermetallic layers. This procedure is costly, time-consuming and does not always produce satisfactory results. Plating must therefore be avoided wherever possible.

It should be noted that the full absence of the intermetallics between dissimilar metals or alloys must not necessarily be considered as a guarantee of their reliable joining. Their absence may be due to the lack of contact between the dissimilar metals, or because of the presence of oxide films, surface contaminations, etc., that excludes any chemical reaction. Clearly, if no reaction occurs, no strong joining of the materials is possible. Therefore, in practice the concept of a permissible intermetallic-layer thickness is essential. This is the maximum thickness of the intermetallic layer which still does not affect noticeably the mechanical strength of the joint. At the same time, the presence of the layer provides evidence for the occurrence of chemical interaction between joined materials. For different pairs of metals and alloys, the permissible intermetallic-layer thickness may vary in the range 0.5–5 μm. Its precise value for each particular couple can only be found experimentally. Once it is known, the parameters of the joining process may be determined on the basis of the layer thickness-time dependence (the so-called growth law of the layer).

Commercial chromium steels usually contain 8 to 29 mass% Cr. To model their behaviour in contact with liquid aluminium, use was made of two iron-chromium

alloys, with a chromium content of 10 and 25 mass%. Experimental data on the dissolution kinetics of the solid-alloy base in the aluminium melt at 700°C were presented in Part I of this contribution [1]. Part II is devoted to the study of the phase identity, chemical composition, morphology and growth kinetics of the intermetallic-compound layers at the alloy-aluminium interface. The effect of dissolution on the layer-growth rates will also be demonstrated.

2. Experimental procedure

2.1. Materials, alloys and specimens

The starting materials used for the investigation were pure metals: powder of carbonyl iron (99.98 mass% Fe), platelets of electrolytic-grade chromium (99.98 mass% Cr) and an aluminium slab (99.995 mass% Al). The iron-chromium alloys were prepared under argon in a conventional arc-melting furnace with a non-consumable tungsten electrode and a water-cooled copper mould, and then cast into 13 mm inner diameter (i.d.) and 100 mm high massive copper crucibles. The ingots were re-melted a few times to ensure their homogeneity. Chromium contents of the Fe–Cr alloy samples were found by chemical analysis and electron probe microanalysis to correspond to the nominal values of 10 and 25 mass% Cr within ± 0.5 mass% (see [1]).

Cylindrical specimens, 11.28 ± 0.01 mm diameter (1.00 cm^2 disc area) and around 5 mm high, were machined from the Fe–Cr alloy rods. The disc surfaces were ground flat and polished mechanically. Prior to the start of the experiment, the alloy specimen was rinsed in ethanol and dried. It was then either attached to (in experiments with saturated aluminium melts), or pressed into (in experiments with undersaturated aluminium melts), a high-purity graphite tube holder.

2.2. Methods

The experimental procedure did not differ from that described in detail in previous works [2, 3]. The runs were carried out at a temperature of 700°C in air under a protective flux. Use was made of a quenching device allowing the experimental cell comprising an alumina crucible (26 mm i.d.), a solid Fe–Cr alloy specimen and the aluminium melt to be cooled down to room temperature in a few seconds by immersing it into a water bath disposed beneath an electric-resistance furnace.

To elucidate the effect of dissolution of the alloy base on the process of formation of intermetallic compounds, two sets of experiments were carried out at 700°C and a dipping time of 100 to 3600 s. In the first set, the saturated aluminium melts were used. In the second, pure aluminium was the starting melt material. In the latter case, the Fe–Cr disc specimens were rotated in the liquid-metal phase (10 cm^3 volume) at an angular speed of 24.0 rad s^{-1}.

The saturated aluminium melts were prepared previously by melting the appropriate amounts of aluminium and a corresponding Fe–Cr alloy (with 10 or 25 mass% Cr), either in an arc furnace in an atmosphere of argon or in an electric-resistance furnace under a flux. Compositions of the saturated Al–Fe–Cr solutions were calculated using the values of the saturation concentrations presented in Part I.

To carry out the experiment, pieces of pure aluminium or an Al–Fe–Cr alloy were first melted under a molten flux. In the case of saturated melts, the liquid was held at a temperature of around 750°C for 900 s to allow the intermetallic phases present in the Al–Fe–Cr alloys to dissolve. In the case of undersaturated melts, this procedure was waived. Then, the Fe–Cr specimen, being rotated at an angular speed of 6.45 rad s^{-1}, was pre-heated in the flux column above the surface of the aluminium melt for approximately 600 s to reach the required temperature of 700°C. This time proved sufficient for the saturation concentrations of iron and chromium in aluminium to be attained.

During the run, the temperature of the liquid phase was maintained to within ±2°C, except at its start when the deviations were sometimes as large as ±5°C. Temperature measurements were carried out using standard Pt–Pt(Rh) and chromel–alumel thermocouples.

When the temperature had equilibrated at 700°C, the Fe–Cr specimen was lowered in the bulk of the aluminium melt and held there for a pre-determined period of time. During isothermal holding in saturated melts, it was not rotated because natural convection was sufficiently strong to prevent the liquation. In this case, all the surface of the Fe–Cr cylindrical specimen was in contact with the melt. In the case of pure aluminium, the specimen was rotated in the melt at an angular speed of 24.0 rad s^{-1}. Its lateral surface was protected with a graphite tube, so that only the disc surface was open for the interaction to proceed.

After holding the Fe–Cr specimen in the aluminium melt for a pre-determined period of time, the crucible (together with the flux, the melt and the specimen) was rapidly immersed into water to arrest the reactions at the alloy-aluminium interface. The Al + (Fe–Cr) specimen obtained was cut along the cylindrical axis, ground flat and polished electrolytically.

The cross-sections prepared in such a way were examined metallographically. The microstructure of the intermetallic-compound layers formed in the transition zone between an iron-chromium alloy and aluminium was observed by optical microscope and scanning electron microscope. Phase identification was carried out by X-ray diffraction. Chemical composition of the intermetallics was determined by electron probe microanalysis (EPMA). Use was made of Jeol Superprobe 733 and CAMECA Camebax SX50 microanalyzers. The spot diameter and the phase volume analyzed at each point were estimated to be 1.5 to 2 μm and 2 to 3 μm^3, respectively. In most cases, EPMA measurements were carried out a few times on the same specimen. As a rule, the sets of the data thus obtained agreed to within ± 0.5 at.%.

3. Results and discussion

3.1. Microstructure, phase identity and chemical composition of the intermetallic-compound layers

Typical microstructures of the alloy-aluminium transition zone are shown in Fig. 1 for a 90 mass%

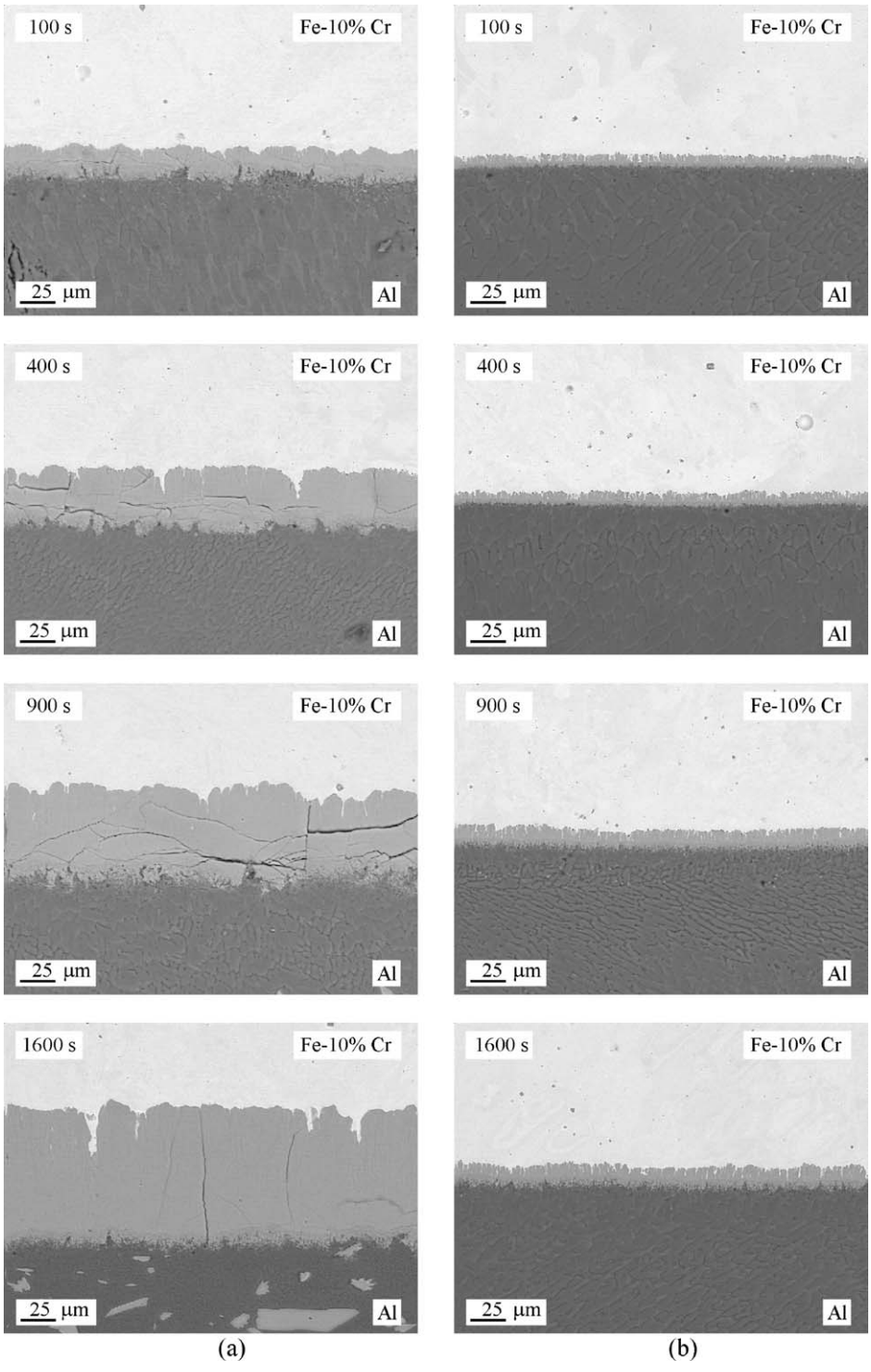

Figure 1 Typical microstructures of the alloy-aluminium transition zone for a 90 mass% Fe–10 mass% Cr alloy at a temperature of 700°C. Initial liquid phase: (a) aluminium saturated with the alloy constituents and (b) pure aluminium ($\omega = 24.0$ rad s^{-1}).

Fe–10 mass% Cr alloy and in Fig. 2 for a 75 mass% Fe–25 mass% Cr alloy. In each case, two sets of micrographs (with saturated and undersaturated melts) are presented to visualize the effect of dissolution on the process of intermetallic compound-layer formation.

Generally, two intermetallic layers were found to form at the alloy-aluminium interface, namely, a compact uniform layer adherent to the alloy base and a porous non-uniform layer bordering with aluminium (Fig. 3). In many cases, the latter actually consisted of separate grains weakly linked or not linked at all with each other. This means that, whenever present, its formation might be partly a result of a solid-state chemical reaction and partly a consequence of crystallization from the melt. On the contrary, the layer adjacent to the alloy base was formed exclusively in the course of another solid-state chemical reaction.

To identify the intermetallic phases, X-ray patterns were taken from different sections of the intermetallic layers. Experimental values of the interplanar distances were compared with those available in the literature for the intermetallics of the Al–Fe and Al–Cr systems [4, 5]. As seen from the X-ray data of Table I, two main

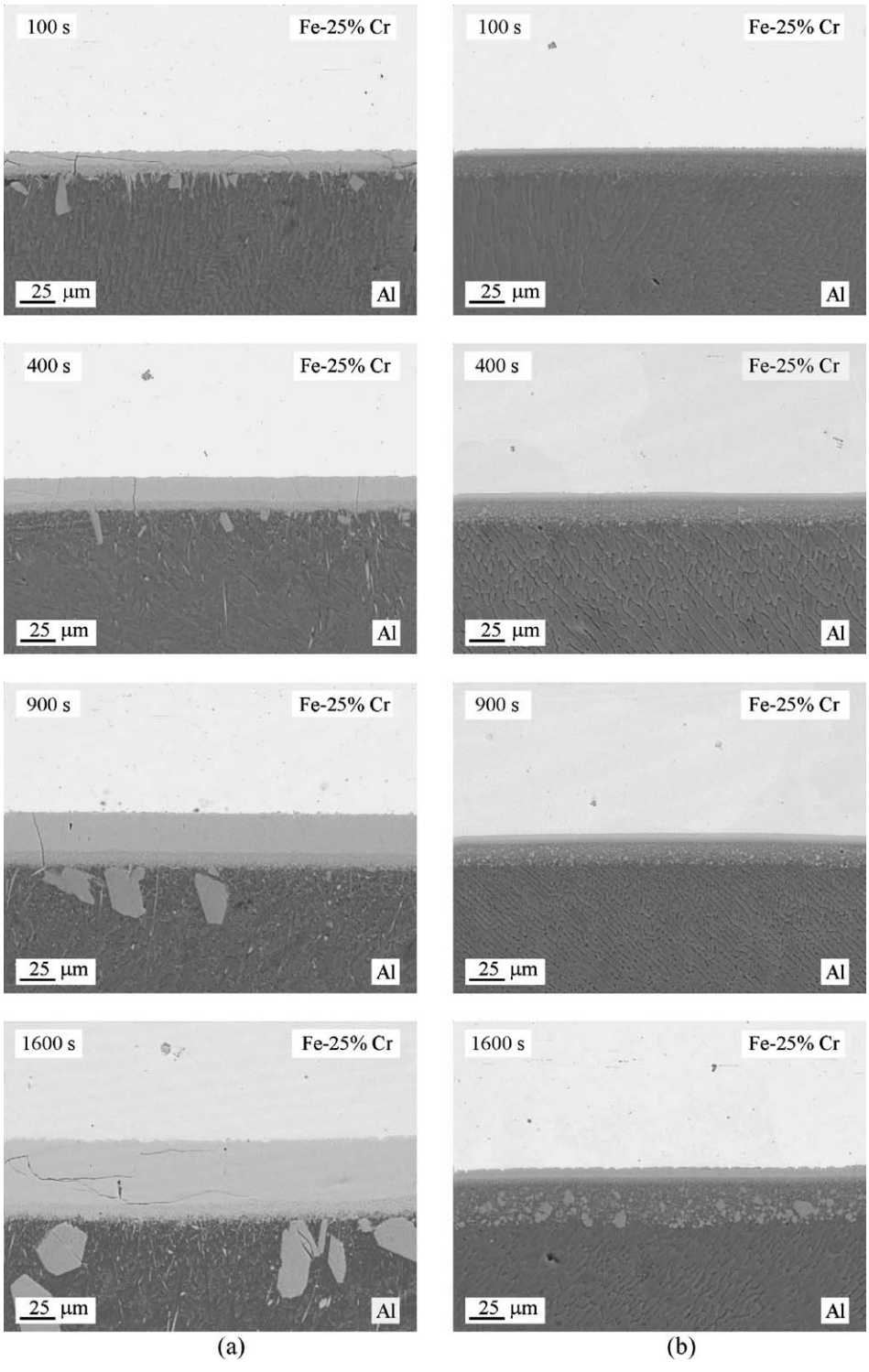

Figure 2 Typical microstructures of the alloy-aluminium transition zone for a 75 mass% Fe–25 mass% Cr alloy at a temperature of 700°C. Initial liquid phase: (a) aluminium saturated with the alloy constituents and (b) pure aluminium ($\omega = 24.0$ rad s^{-1}).

constituent phases were Fe_2Al_5 and $FeAl_3$, with the compact layer being the Fe_2Al_5 phase, and the porous layer the $FeAl_3$ phase. The latter is often designated Fe_2Al_7 [6–9]. As will be seen later, this designation is more appropriate in the case under consideration. It should be noted that X-ray patterns of the porous layer also contained a number of unidentifiable, very weak diffraction peaks, indicative of the presence of other intermetallic compounds.

To reveal the phase compositions, EPMA measurements were carried out across the transition zone up to a depth of 100 μm into the alloy bulk and 100 μm into the aluminium bulk. Tables II to V, in which only about one-fifth of all the measurements performed are presented, summarize in the most general features the results obtained. The phases for which the identification is ambiguous are indicated with a question mark.

The composition of the compact layer (Fig. 3) is seen to correspond to that of the Fe_2Al_5 phase (28.6 at.% Fe, 71.4 at.% Al). A change of elemental content across its thickness (69.0–72.9 at.% Al) agrees fairly well with the width (70.0–72.5 at.% Al) of the homogeneity range of this intermetallic compound in the equilibrium phase diagram of the Al–Fe binary system [6, 10].

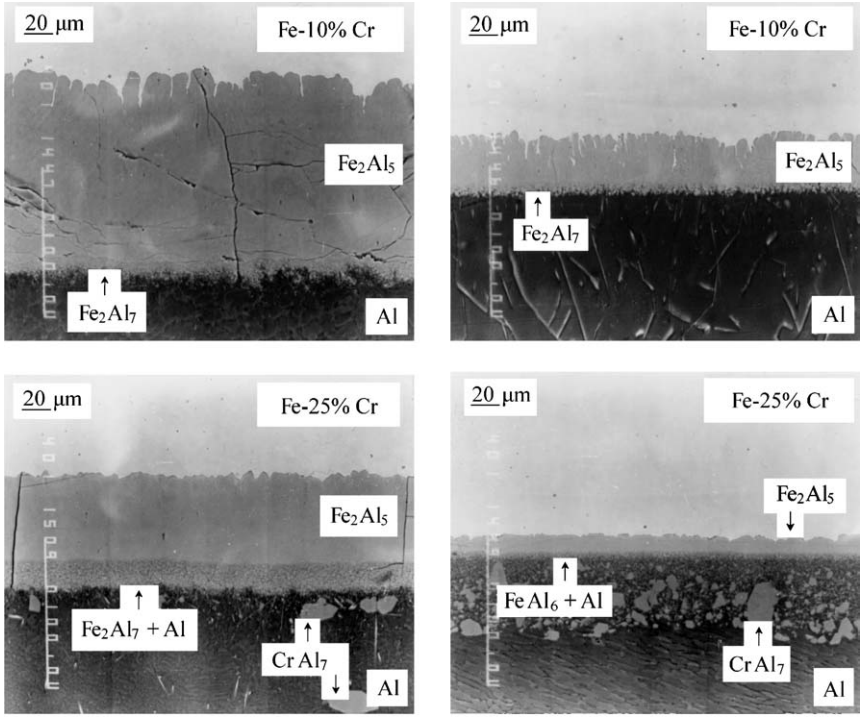

Figure 3 Microstructures of the Fe–Cr alloy-aluminium transition zone at a temperature of 700°C and a dipping time of 3600 s. Initial liquid phase: (a) aluminium saturated with the alloy constituents and (b) pure aluminium ($\omega = 24.0$ rad s^{-1}).

Somewhat lower aluminium contents (not listed) at some places near the Fe_2Al_5-alloy interface are easily explainable. When carrying out the EPMA measurements, it was noticed that, wherever cracks stretching along the intermetallic layer were present (see Fig. 3a), the aluminium content dropped very considerably, even down to the composition of the adjacent phase $FeAl_2$. This may be illustrated by the following two sets of aluminium percentage (at.%) obtained on a "75 mass% Fe–25 mass% Cr alloy + saturated aluminium" specimen (700°C, 3600 s):

without a crack 69.11 69.12 69.35 69.47 70.08 70.99 71.68 71.99 72.23 72.50

with a crack <u>65.04</u> <u>65.05</u> <u>65.26</u> <u>65.85</u> <u>66.18</u> 69.07 70.27 70.51 71.06 71.36

TABLE I Experimental intensities of X-ray reflections and interplanar spacings, d, for the intermetallic compounds present in the transition zone between a 75 mass% Fe–25 mass% Cr alloy and saturated or undersaturated aluminium. The compositional data in Tables II–V indicate that it is more appropriate to designate the $FeAl_3$ phase as Fe_2Al_7

Intensity	d_{exp} (nm)	$Al_{saturated}$		$Al_{undersaturated}$	
m	0.318	Fe_2Al_5		Fe_2Al_5	
m	0.234		$FeAl_3$		
vs	0.210	Fe_2Al_5	$FeAl_3$	Fe_2Al_5	$FeAl_3$
vs	0.205	Fe_2Al_5	$FeAl_3$	Fe_2Al_5	$FeAl_3$
s	0.202		$FeAl_3$		$FeAl_3$
w	0.195	Fe_2Al_5	$FeAl_3$	Fe_2Al_5	$FeAl_3$
w	0.191	Fe_2Al_5		Fe_2Al_5	
vw	0.184			Fe_2Al_5	
w	0.176	Fe_2Al_5		Fe_2Al_5	
vw	0.156			Fe_2Al_5	
m	0.1481	Fe_2Al_5		Fe_2Al_5	
vw	0.1444		$FeAl_3$		
w	0.1420	Fe_2Al_5		Fe_2Al_5	
w	0.1390	Fe_2Al_5	$FeAl_3$	Fe_2Al_5	$FeAl_3$
vw	0.1348	Fe_2Al_5	$FeAl_3$	Fe_2Al_5	$FeAl_3$
vw	0.1300	Fe_2Al_5	$FeAl_3$	Fe_2Al_5	$FeAl_3$
w	0.1272	Fe_2Al_5	$FeAl_3$	Fe_2Al_5	$FeAl_3$
m	0.1255		$FeAl_3$		$FeAl_3$
m	0.1229		$FeAl_3$		$FeAl_3$
m	0.1219	Fe_2Al_5	$FeAl_3$	Fe_2Al_5	$FeAl_3$
vw	0.1175	Fe_2Al_5	$FeAl_3$	Fe_2Al_5	$FeAl_3$
vw	0.1090	Fe_2Al_5		Fe_2Al_5	
w	0.1064	Fe_2Al_5		Fe_2Al_5	
vw	0.1039	Fe_2Al_5		Fe_2Al_5	
vw	0.1023	Fe_2Al_5		Fe_2Al_5	

Intensity: vs = very strong, s = strong, m = medium, w = weak, vw = very weak.

In both cases, the measurements were made at a step of 2 μm, starting from the alloy-intermetallic layer interface. Underlined values evidently represent the aluminium content of $FeAl_2$, though this phase does not form a continuous layer. The mechanism of its formation is as follows. The crack separates some part of the Fe_2Al_5 layer from its main body. As a result, a new reaction couple consisting of an iron-chromium alloy and the Fe_2Al_5 phase is formed. The formation of the $FeAl_2$ intermetallic compound in this couple is due to two chemical reactions (see [3]), namely $Fe_2Al_5 = 2FeAl_2 + Al_{dif}$ and $2Al_{dif} + Fe = FeAl_2$.

It is worth noting that the appearance of cracks in the course of growth of intermetallic-compound layers in any reaction couple is unavoidable. Their formation is due mainly to the volume effect and the difference of thermal expansion coefficients of the couple constituents. After the cracks form, the initial reaction couple splits into a few independent couples. In those couples, additional phases missing from the initial one can readily occur, giving rise to a complicated multiple-layer microstructure of the transition zone. Caution is

TABLE II Electron probe microanalysis data for the transition zone between a 90 mass% Fe–10 mass% Cr alloy and saturated aluminium. Temperature 700°C, annealing time 3600 s

Phase	Place of measurement	Content (at.%) Al	Fe	Cr	Remarks
	At distance l away from the interface between a Fe—Cr alloy and an adjacent intermetallic layer				
Fe—Cr	$l = -100$ μm	0.015	88.67	11.32	
	−50	0.027	88.40	11.57	
	−15	0.000	88.44	11.56	
	−10	0.059	88.49	11.46	
	−5	0.092	88.49	11.42	
Fe—Cr-bordering intermetallic layer	5	71.76	25.18	3.06	Fe_2Al_5
	20	72.07	24.80	3.13	
	35	72.26	24.52	3.22	
	50	72.17	24.92	2.91	
	65	72.30	24.56	3.14	
	80	72.48	24.39	3.13	
	95	72.34	24.56	3.10	
	110	72.32	24.63	3.05	
	125	72.45	24.32	3.13	
	140	72.64	24.07	3.29	About 5 μm away from the end of the intermetallic layer
Al-bordering intermetallic layer	Middle part of the layer, at random	77.95	21.30	0.75	Fe_2Al_7
		77.62	21.48	0.90	
		77.78	21.09	1.13	
		76.76	22.09	1.15	
		75.47	22.24	2.29	$FeAl_3$
		72.58	24.78	2.64	Fe_2Al_5
	At distance l away from the Al-bordering intermetallic layer				
Al	$l = 5$ μm	98.11	1.68	0.21	⟨Al⟩
	10	99.15	0.67	0.18	
	25	98.95	0.88	0.17	
	50	99.03	0.80	0.17	
	100	98.33	1.51	0.16	

therefore necessary in interpreting the data of reaction-diffusion experiments because it is not always possible to decide unambiguously whether the formation of a given compound is a result of a primary or a secondary process.

EPMA measurements showed the porous layer to consist of grains of Fe_2Al_7 or $FeAl_6$, with an aluminium solid solution between them. The layer also contained inclusions of $FeAl_3$ and occasionally Fe_2Al_5.

The coarse grains in the vicinity of the Fe—Cr alloy-aluminium interface are the $CrAl_7$ phase, also designated Cr_2Al_{13} or Cr_7Al_{45}, with the homogeneity range 86.3–87.6 at.% Al [11] or 87.3–88.5 at.% Al [10]. It is worth mentioning that, when formed under non-equilibrium conditions, this phase has a composition closer to $CrAl_6$ than to $CrAl_7$. In the presence of a third metal (Fe, Mn, etc.), the $CrAl_6$ phase is known to give rise to a few metastable phases with five-fold symmetry [12] whose composition corresponds to the chemical formula $Cr_{0.7}Fe_{0.3}Al_6$.

Fine grains near the Fe_2Al_5 layer had an approximate composition of $Cr_{0.67}Fe_{0.33}Al_{13}$. With increasing distance from this layer towards aluminium, their size increased, while the composition approached $CrAl_7$. The observed phase sequence and composition profile is probably a result of the series of transformations, namely $Cr_{0.67}Fe_{0.33}Al_{13} \rightarrow Cr_{0.7}Fe_{0.3}Al_6 \rightarrow CrAl_6 \rightarrow CrAl_7$. As seen from Table V, the iron solubility in the latter phase reaches 4 at.%.

3.2. Growth kinetics of the intermetallic-compound layers in the case of the saturated aluminium melt

The layer thickness-time dependences for the Fe—Cr alloys and the saturated aluminium melt are shown graphically in Fig. 4, while the numerical data are presented in Tables VI and VII. In the case of a 90 mass% Fe–10 mass% Cr alloy, the thickness of the compact layer is seen to increase in the 100–3600 s time range from 14 μm to about 128 μm, while that of the porous layer increases from 8 μm to about 13 μm. For a 75 mass% Fe–25 mass% Cr alloy, appropriate values are 12–60 μm and 4–12 μm.

Though the growth kinetics of two compound layers are traditionally assumed to be parabolic [13], this is not the case with many systems, including the system under investigation. Instead, a few kinetic laws

TABLE III Electron probe microanalysis data of the transition zone between a 75 mass% Fe–25 mass% Cr alloy and saturated aluminium. Temperature 700°C, annealing time 3600 s

Phase	Place of measurement	Content (at.%) Al	Fe	Cr	Remarks
	At distance l away from the interface between a Fe—Cr alloy and an adjacent intermetallic layer				
Fe—Cr	$l = -100$ μm	0.013	73.83	26.15	
	−50	0.046	73.98	25.97	
	−15	0.041	73.29	11.56	
	−10	0.015	73.02	26.96	
	−5	0.000	73.33	26.67	
Fe—Cr-bordering intermetallic layer	5	69.11	21.75	9.13	Fe_2Al_5
	15	69.47	21.72	8.81	
	25	70.08	21.28	8.64	
	35	71.68	20.11	8.22	
	45	72.50	19.97	7.53	
	60	72.91	20.15	6.94	About 3 μm away from the end of the intermetallic layer
Al-bordering intermetallic layer	Middle part of the layer, at random	77.34	21.59	1.02	Fe_2Al_7
		76.72	21.88	1.40	
		79.30	19.61	1.09	
		77.57	21.12	1.31	
		78.05	20.84	1.11	
		72.47	19.56	7.97	Fe_2Al_5
		74.84	17.59	7.57	$FeAl_3$
	At distance l away from the Al-bordering intermetallic layer				
Al	$l = 5$ μm	98.80	0.96	0.24	⟨Al⟩
	10	99.19	0.58	0.23	
	25	98.70	1.07	0.23	
	50	99.12	0.68	0.20	
	100	98.75	1.05	0.20	

(linear, paralinear, asymptotic, etc.) may be observed for one and the same system at sufficiently long times of interaction [3], and only relatively small portions of the layer thickness-time dependence are close to a parabola. In the case under consideration, a parabolic relation of the type $x^2 = 2k_1t$ does not seem to produce a satisfactory agreement with the experimental data (Tables VI and VII) because k_1 does not remain constant except $k_{1(\text{total})}$ in Table VI and perhaps $k_{1(\text{compact layer})}$ in Table VII. Moreover, this relation cannot be applied at all to the porous layer whose thickness quickly (in about 400 s) reaches a certain value and then remains practically unchanged during a considerable period of time. Such a dependence cannot be explained in a purely diffusional framework predicting only parabolic kinetics for all growing layers but seems to be quite natural in the framework of physicochemical views giving a variety of growth laws (for more detail, see [3]).

3.3. The effect of dissolution on the intermetallic layer-growth rate and its mathematical description

The effect of dissolution on the process of intermetallic compound-layer formation is visualized in Fig. 4 where two sets of micrographs with the saturated (a) and undersaturated (b) melt are presented, and in Fig. 5 where the layer thickness-time dependences are shown. Dissolution is seen to cause a three-fold decrease in layer thickness compared to the case above where the Fe—Cr alloy is in contact with a saturated melt and no dissolution occurs. Note that under conditions of simultaneous dissolution only the compact Fe_2Al_5 layer survives, whereas other intermetallic phases ($FeAl_6$, Fe_2Al_7, $FeAl_3$) exist as separate inclusions in the aluminium matrix.

The total change in thickness of the Fe_2Al_5 layer during a small period of time, dt, is equal to the difference between the rates of its growth and dissolution. The dissolution rate is

$$\frac{dx_d}{dt} = b_t = b_0 \exp(-at) \tag{1}$$

where

$$b_0 = \frac{c_s k}{\rho_{int}\varphi}, \quad a = \frac{kS}{v},$$

c_s is the saturation concentration or solubility of iron in aluminium at 700°C, k is the dissolution rate constant,

TABLE IV Electron probe microanalysis data of the transition zone between a 90 mass% Fe–10 mass% Cr alloy and undersaturated aluminium. Temperature 700°C, annealing time 3600 s, rotational speed 24.0 rad s^{-1}

Phase	Place of measurement	Content (at.%) Al	Fe	Cr	Remarks
	At distance l away from the interface between a Fe—Cr alloy and an adjacent intermetallic layer				
Fe—Cr	$l = -100$ μm	0.123	89.08	10.80	
	−50	0.095	88.84	11.06	
	−15	0.059	89.11	10.83	
	−10	0.132	89.07	10.80	
	−5	0.093	89.02	10.88	
Fe—Cr-bordering intermetallic layer	5	72.19	24.72	3.09	Fe_2Al_5
	10	72.28	24.75	2.97	
	15	72.34	24.62	3.04	
	20	72.37	24.71	2.92	
	25	72.38	24.52	3.10	
	30	72.39	24.66	2.95	
	35	72.48	24.44	3.07	
	40	72.97	24.05	2.98	About 2 μm away from the end of the intermetallic layer
Grains in Al near the Fe_2Al_5 layer	Along the Fe_2Al_5–Al interface, at random	77.53	20.62	1.85	Fe_2Al_7
		76.62	21.42	1.96	
		78.43	20.00	1.57	
		77.84	21.04	1.12	
		79.84	19.13	1.03	
		72.62	24.51	2.87	Fe_2Al_5
		75.43	22.02	2.55	$FeAl_3$
		84.08	14.99	0.93	$FeAl_6$?
	At distance l away from the Fe_2Al_5 layer				
Al	$l = 5$ μm	99.58	0.28	0.14	⟨Al⟩
	10	99.71	0.16	0.13	
	25	99.75	0.11	0.14	
	50	99.79	0.10	0.11	
	100	99.84	0.08	0.08	

ρ_{int} is the density of the intermetallic compound Fe_2Al_5, φ is the content of Fe in Fe_2Al_5, S is the surface area of the solid in contact with the liquid, and v is the volume of the liquid phase.

Though a general mathematical equation describing the intermetallic layer-growth kinetics under conditions of its simultaneous dissolution in the liquid phase is rather complicated and difficult to solve [3], in the case under consideration it assumes a simpler form suitable for estimating the layer thickness, namely:

$$x_t = k_1/b_t \quad (2)$$

where k_1 is the layer growth-rate constant and x_t is the maximum thickness that can be reached by the growing intermetallic layer in time t if the rate of its dissolution remains constant and equal to b_t in the time range 0–t.

When employing Equation 2, the main difficulty to overcome is evaluating the layer growth-rate constant, k_1. If a single-phase intermetallic layer occurs in the case of both saturated and undersaturated melts, its value is readily found from the experimental layer thickness-time dependence for the saturated melt. With the Fe—Cr alloys investigated here, however, this is not possible since the number of intermetallic layers growing from saturated and undersaturated melts is different (two, namely Fe_2Al_5 and Fe_2Al_7 in the case of the saturated aluminium melt, and only one, Fe_2Al_5, from the undersaturated melt). Therefore, the layer-growth constant, k_1, can only be calculated using a few experimentally determined points of the layer thickness-time dependence for the undersaturated melt, preferably at short times. This makes the calculation of other points of that dependence possible.

Since the dissolution rate diminishes exponentially from b_0 to b_t in the time range 0–t, calculations were carried out twice for each point by putting in the denominator of Equation 2 first equal to $(b_0 + b_t)/2$ and then b_t. Thus, two sets of the Fe_2Al_5 layer thickness were obtained. The first set represents the underestimated values, x_{under}, whereas the second set gives the overestimated ones, x_{over}. Experimental values, x_{exp}, must clearly lie somewhere in between. For both alloys, the layer growth-rate constant, k_1, was calculated from Equation 2 using the first two points $t = 100$ s and $t = 225$ s, with $x_{exp} = 9 \times 10^{-6}$ m and $x_{exp} = 10 \times 10^{-6}$ m for a 90 mass% Fe–10 mass% Cr alloy and $x_{exp} = 5.0 \times 10^{-6}$ m and $x_{exp} = 5.2 \times 10^{-6}$ m for a 75 mass% Fe–25 mass% Cr alloy. Appropriate values of k_1 were found to be 14.1×10^{-12} m^2 s^{-1}

TABLE V Electron probe microanalysis data of the transition zone between a 75 mass% Fe–25 mass% Cr alloy and undersaturated aluminium. Temperature 700°C, annealing time 3600 s, rotational speed 24.0 rad s^{-1}

Phase	Place of measurement	Content (at.%)			Remarks
		Al	Fe	Cr	
	At distance l away from the interface between a Fe—Cr alloy and an adjacent intermetallic layer				
Fe—Cr	$l = -100$ μm	0.000	73.21	26.79	
	−50	0.059	73.24	26.70	
	−15	0.000	73.00	27.00	
	−10	0.000	73.21	26.79	
	−5	0.148	73.53	26.32	
Fe—Cr-bordering intermetallic layer	3	68.88	22.20	8.92	Fe_2Al_5
	5	70.48	21.09	8.43	
	7	71.22	20.63	8.15	
	9	72.23	20.16	7.61	
	11	72.91	19.54	7.55	About 2 μm away from the end of the intermetallic layer
Grains in Al near the Fe_2Al_5 layer	Along the Fe_2Al_5–Al interface, at random	85.16	9.97	4.87	$FeAl_6$
		86.00	10.33	3.67	
		85.70	9.26	5.04	
		86.57	9.27	4.16	
		92.89	2.00	4.10	$Cr_{0.67}Fe_{0.33}Al_{13}$?
		92.93	2.16	4.91	
		92.38	1.84	5.78	
Coarse grains in Al		87.53	4.08	10.50	$CrAl_7$
		85.46	2.43	12.11	
		87.49	2.29	10.22	
		85.88	2.22	11.90	
		86.98	1.99	11.03	
	At distance l away from the Fe_2Al_5 layer				
Al	$l = 5$ μm	99.45	0.31	0.24	⟨Al⟩
	10	99.46	0.31	0.23	
	25	99.18	0.61	0.21	
	50	99.59	0.18	0.23	
	100	99.37	0.39	0.24	

TABLE VI Thicknesses, x, of the intermetallic layers and calculated diffusional constants, $k_1 = x^2/2t$, for a 90 mass% Fe–10 mass% Cr alloy and the saturated aluminium melt at a temperature of 700°C

Time (s)	x_{total} ($\times 10^{-6}$ m)	$k_{1(total)}$ ($\times 10^{-12}$ m^2 s^{-1})	$x_{compact\ layer}$ ($\times 10^{-6}$ m)	$k_{1(compact\ layer)}$ ($\times 10^{-12}$ m^2 s^{-1})	$x_{porous\ layer}$ ($\times 10^{-6}$ m)
100	22	2.4	14	1.0	8
225	34	2.6	24	1.3	10
400	42	2.2	30	1.1	12
625	56	2.5	43	1.5	13
900	64	2.3	50	1.4	14
1225	76	2.4	63	1.2	13
1600	88	2.4	75	1.8	13
3600	140	2.7	128	2.3	12

TABLE VII Thicknesses, x, of the intermetallic layers and calculated diffusional constants, $k_1 = x^2/2t$, for a 75 mass% Fe–25 mass% Cr alloy and the saturated aluminium melt at a temperature of 700°C

Time (s)	x_{total} ($\times 10^{-6}$ m)	$k_{1(total)}$ ($\times 10^{-12}$ m^2 s^{-1})	$x_{compact\ layer}$ ($\times 10^{-6}$ m)	$k_{1(compact\ layer)}$ ($\times 10^{-12}$ m^2 s^{-1})	$x_{porous\ layer}$ ($\times 10^{-6}$ m)
100	16	1.3	12	0.7	4
225	28	1.7	20	0.9	8
400	32	1.3	22	0.6	10
625	36	1.0	26	0.5	10
900	40	0.9	30	0.5	10
1600	52	0.8	42	0.6	10
3600	72	0.7	60	0.5	12

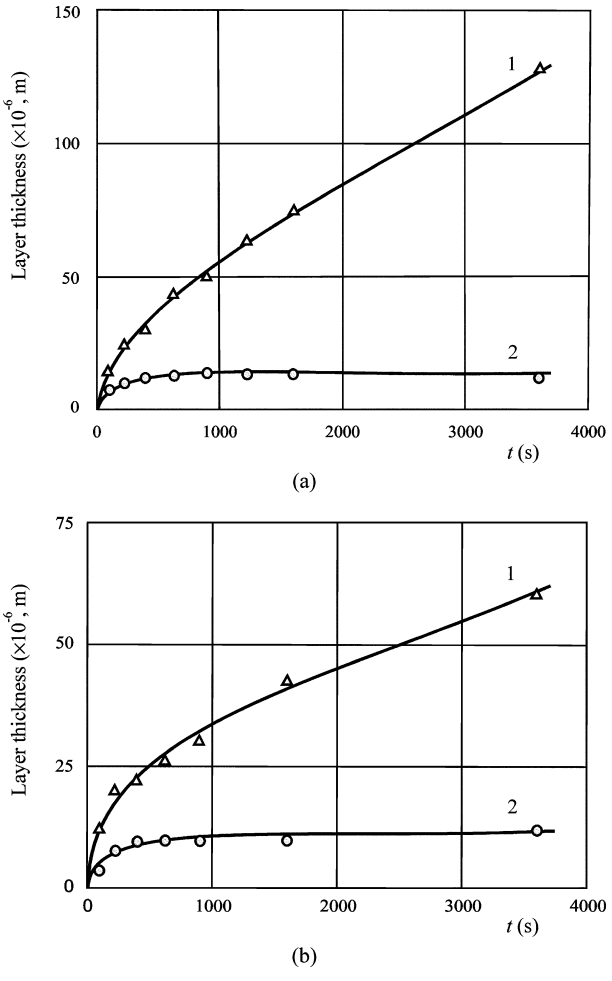

Figure 4 Layer thickness as a function of time for the Fe—Cr alloys and the saturated aluminium melt at a temperature of 700°C. 1, intermetallic layer adherent to the alloy base; 2, intermetallic layer bordering with aluminium: (a) 90 mass% Fe–10 mass% Cr alloy and (b) 75 mass% Fe–25 mass% Cr alloy.

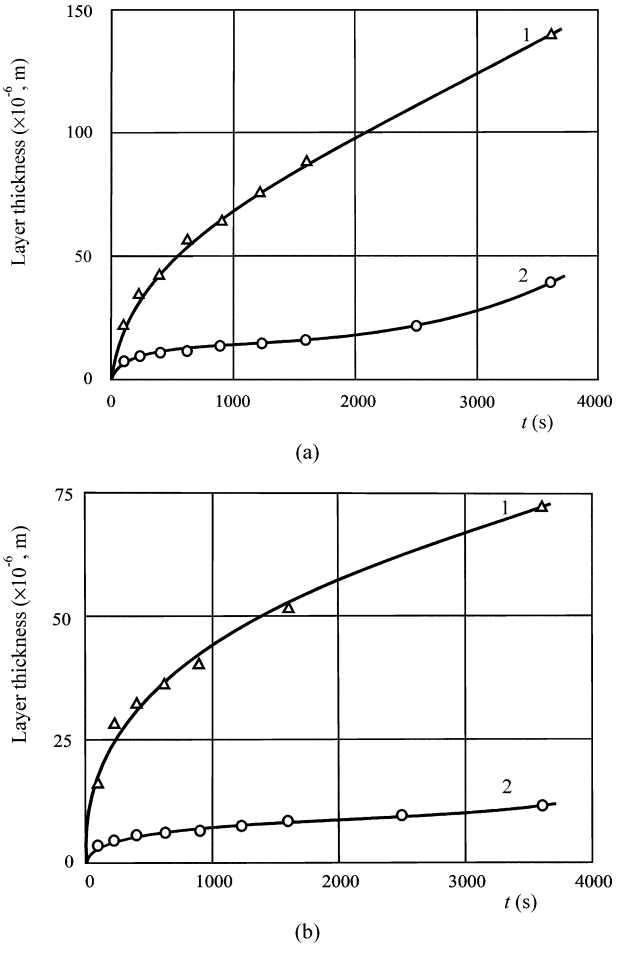

Figure 5 Layer thickness as a function of time for the Fe—Cr alloys and the aluminium melt at a temperature of 700°C. 1, total thickness of both intermetallic layers Fe_2Al_5 and Fe_2Al_7 in the case of the saturated aluminium melt; 2, thickness of the intermetallic layer Fe_2Al_5 (Fe_2Al_7 is missing) in the case of the undersaturated aluminium melt ($\omega = 24.0$ rad s^{-1}): (a) 90 mass% Fe–10 mass% Cr alloy and (b) 75 mass% Fe–25 mass% Cr alloy.

and 5.5×10^{-12} m^2 s^{-1}. These are the average of b_0x_{100} and $b_{100}x_{225}$ (subscripts designate time). Other necessary quantities were as follows.

90 mass% Fe–10 mass% Cr alloy:

$$k = 4.2 \times 10^{-5}\,\mathrm{m\,s^{-1}}[1]$$

$$c_s = 66.72\,\mathrm{kg\,m^{-3}}(2.5\,\mathrm{mass\%Fe} + 0.28\,\mathrm{mass\%Cr}\,[1])$$

$$a = 4.2 \times 10^{-4}\,\mathrm{s^{-1}}$$

$$b_0 = 1.51 \times 10^{-6}\,\mathrm{m\,s^{-1}}$$

75 mass% Fe–25 mass% Cr alloy:

$$k = 3.0 \times 10^{-5}\,\mathrm{m\,s^{-1}}[1]$$

$$c_s = 70.08\,\mathrm{kg\,m^{-3}}(2.2\,\mathrm{mass\%Fe} + 0.72\,\mathrm{mass\%Cr}\,[1])$$

$$a = 3.0 \times 10^{-4}\,\mathrm{s^{-1}}$$

$$b_0 = 1.13 \times 10^{-6}\,\mathrm{m\,s^{-1}}$$

The final results are presented in Tables VIII and IX. Equation 2 is seen to produce a satisfactory

TABLE VIII Calculated and experimental thicknesses, x, of the Fe_2Al_5 intermetallic layer for a 90 mass% Fe–10 mass% Cr alloy and the undersaturated aluminium melt at a temperature of 700°C and $\omega = 24.0$ rad s^{-1}

Time (s)	$(b_0 + b_t)/2$ ($\times 10^{-6}$ m s^{-1})	x_{under} ($\times 10^{-6}$ m)	b_t ($\times 10^{-6}$ m s^{-1})	x_{over} ($\times 10^{-6}$ m)	x_{exp} ($\times 10^{-6}$ m)
100	1.48		1.45		9.0
225	1.44		1.37		10.0
400	1.39	10.1	1.28	11.0	11.0
625	1.33	10.6	1.16	12.2	12.0
900	1.27	11.1	1.03	13.7	13.5
1225	1.20	11.8	0.90	15.7	15.0
1600	1.14	12.4	0.77	18.3	16.0
2500	1.02	13.8	0.53	26.6	22.5
3600	0.92	15.3	0.33	42.7	40.0

TABLE IX Calculated and experimental thicknesses, x, of the Fe_2Al_5 intermetallic layer for a 75 mass% Fe–25 mass% Cr alloy and the undersaturated aluminium melt at a temperature of 700°C and $\omega = 24.0$ rad s^{-1}

Time (s)	$(b_0 + b_t)/2$ ($\times 10^{-6}$ m s^{-1})	x_{under} ($\times 10^{-6}$ m)	b_t ($\times 10^{-6}$ m s^{-1})	x_{over} ($\times 10^{-6}$ m)	x_{exp} ($\times 10^{-6}$ m)
100	1.11		1.10		5.0
225	1.10		1.06		5.2
400	1.06	5.2	1.00	5.5	5.5
625	1.03	5.3	0.94	5.9	6.0
900	1.00	5.5	0.86	6.4	6.5
1225	0.95	5.8	0.78	7.1	7.0
1600	0.91	6.0	0.70	7.9	8.0
2500	0.83	6.6	0.53	10.4	9.5
3600	0.75	7.3	0.38	14.5	12.0

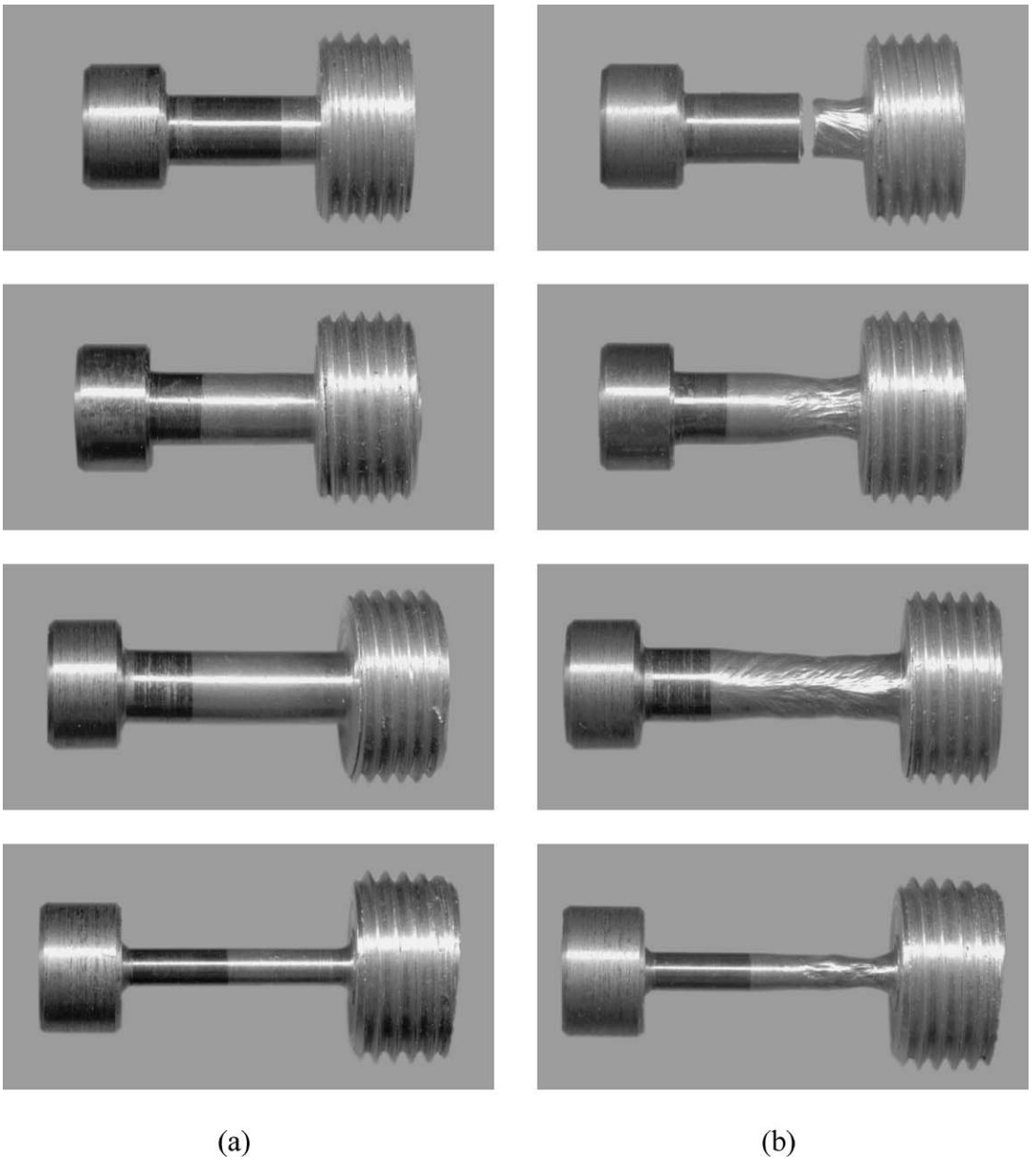

Figure 6 Fe–Cr alloy-to-aluminium transition joints before (a) and after (b) tensile tests.

fit to the experimental data. Note that the intermetallic layer growth-rate constant, k_1, tends to rise slightly with increasing time because of the anisotropy of growth of the Fe_2Al_5 phase [14]. Therefore, as might be expected, the experimental values of the Fe_2Al_5 layer thickness, calculated with the use of a smaller value of this constant determined from the initial points of the layer thickness-time plots, are closer to the overestimated than to underestimated ones.

TABLE X Tensile test results for the Fe–Cr alloy-to-aluminium transition joints

Specimen number	Gauge length -to-diameter ratio	Rupture strength (MPa)	Remarks
5-p (10% Cr)	1:2	79	Failure along the interface after the formation of a neck in the aluminium part of the sample
7-p (10% Cr)	3:2	82	Plastic flow of aluminium with the formation of a neck
8-p (25% Cr)	3:1	78	Plastic flow of aluminium with the formation of a neck
9-p (25% Cr)	3:1	67	Plastic flow of aluminium with the formation of a neck

3.4. Fe–Cr alloy-to-aluminium joining

From Equation 2 and the experimental data obtained, it follows that the intermetallic layer thickness can be reduced to a permissible level of 2–3 μm solely by increasing the dissolution rate of the solid in the liquid phase, without employing any additional technological operations. Use is thus to be made of a welding-soldering process resembling the one of soldering of one metal to another by its own melt. The Fe–Cr alloys can successfully be joined to aluminium by means of interaction of the solid alloy with the aluminium melt under strictly specified conditions of temperature, time and liquid agitation, followed by their joint cooling at a controlled rate until the melt crystallizes. This method of joining is most suitable for making transition joints of cylindrical form, 10–100 mm in diameter and up to 100 mm long. It is applicable not only to this particular combination of materials but to others as well, the constituents of which strongly differ by their melting points.

The Fe–Cr alloy-to-aluminium transition joints, 10–25 mm diameter and 30–35 mm long, were made and their uniaxial tensile tests were carried out on a P-500 tester. The gauge length of the aluminium part was 5–15 mm, while the diameter was 3–6 mm. During the tensile tests, the crosshead speed was 0.1 mm s^{-1}.

As seen from Fig. 6 and Table X, the mechanical strength of the joint is not less than that of pure aluminium. Even with specimens whose gauge length was equal to half the diameter, the rupture occurred along the interface between dissimilar materials only after the plastic deformation of aluminium with the formation of an apparent neck. The rupture strength, σ, was typical of pure aluminium (70–80 MPa). If the gauge length exceeded the diameter, the rupture took place approximately in the middle of the aluminium part of the specimens.

4. Conclusions

At 700°C, two intermetallic layers are formed at the interface between the Fe–Cr alloys containing 10 and 25 mass% chromium and the saturated aluminium melt. The layer adherent to the alloy base is compact and uniform, while that bordering with aluminium is porous and irregular. The former consists of the Fe_2Al_5 phase. The main constituent of the latter is the Fe_2Al_7 phase.

Only the Fe_2Al_5 layer occurs under conditions of simultaneous dissolution of the alloy base in the liquid phase. Its growth kinetics are non-parabolic. An equation taking account of the dissolution process on the growth rate of the intermetallic layer produces a good fit to the experimental data.

Besides Fe_2Al_5 and Fe_2Al_7, other intermetallic phases ($FeAl_3$, $FeAl_6$,$CrAl_7$, $Cr_{0.67}Fe_{0.33}Al_{13}$) are revealed in the aluminium matrix in the vicinity of the Fe–Cr alloy-aluminium interface. Their occurrence is likely to be a result of crystallization from the melt.

The Fe–Cr alloys can be joined to aluminium by means of interaction of the solid alloy with the aluminium melt, followed by their joint cooling until the melt crystallizes. The mechanical strength of the joint is not less than that of pure aluminium.

Acknowledgements

This investigation was supported in part by the STCU grant no. 2028. The help of V. G. Khoruzha, L. A. Duma, V. R. Sidorko, K. A. Meleshevich, A. V. Samelyuk and V. M. Vereshchaka in conducting the experiments and carrying out the necessary analyses is acknowledged with gratitude.

References

1. K. BARMAK and V. I. DYBKOV, *J. Mater. Sci.* **38** (2003) 3249.
2. V. I. DYBKOV, *ibid.* **35** (2000) 1729.
3. *Idem.*, "Reaction Diffusion and Solid State Chemical Kinetics" (The IPMS Publications, Kyiv, 2002) Chap. 5.
4. L. I. MIRKIN, "Spravochnik po rentgenostrukturnomu analizu polikristallov" (Fizmatgiz, Moskwa, 1961) p. 458 (in Russian).
5. S. S. GORELIK, L. N. RASTORGUEV and YU. A. SKAKOV, "Rentgenograficheskiy i elektronno-opticheskiy analiz: prilozheniya" (Metallurgiya, Moskwa, 1970) p. 33 (in Russian).
6. M. HANSEN, "Constitution of Binary Alloys" (McGraw-Hill, New York, 1958) pp. 81, 90.
7. A. E. VOL, "Structura i svoystva binarnikh metallicheskikh system" (Fizmatgiz, Moskwa, 1959) Vol. I, pp. 217, 504 (in Russian).
8. T. B. MASSALSKI, J. L. MURRAY, L. H. BENNETT and H. BAKER (eds.), in "Binary Alloy Phase Diagrams" (American Society for Metals, Metals Park, OH, 1986) Vol. I, pp. 103, 111.
9. L. F. MONDOLFO, "Aluminium Alloys: Structure and Properties" (Butterworths, London-Boston, 1976) pp. 38, 68, 235.
10. G. GHOSH, in "Ternary Alloys: A Comprehensive Compendium of Evaluated Constitutional Data and Phase Diagrams," edited by G. Petzow and G. Effenberg (VCH, Weinheim, 1991) Vol. 4, pp. 324–343.
11. J. L. MURRAY, *J. Phase Equil.* **19** (1998) 368.
12. F. VAN DER WOUDE and P. J. SCHURER, *Canad. J.Phys.* **65** (1987) 1301.
13. K. P. GUROV, B. A. KARTASHKIN and YU. E. UGASTE, "Vzaimnaya diffuziya v mnogofaznykh metallicheskikh sistemakh" (Nauka, Moskwa, 1981) Chap. 6.
14. V. N. YEREMENKO, YA. V. NATANZON and V. I. DYBKOV, *J. Mater. Sci.* **16** (1981) 1748.

Received 18 June 2003
and accepted 8 March 2004